Impacts of higher-order dispersions and saturable nonlinearities on modulation instability in negative-refractive metamaterials*

Zhong Xian-Qiong(钟先琼)†, Cheng Ke(程 科), and Xiang An-Ping(向安平)

College of Optoelectronic Technology, Chengdu University of Information Technology, Chengdu 610225, *China*

(Received 21 July 2012; revised manuscript received 18 September 2012)

On the basis of the standard linear stability analysis and Drude electromagnetic model, the impacts of higher-order dispersions and three kinds of typical saturable nonlinearities on modulation instability (MI) have been analyzed and calculated for negative-refractive metamaterials (MMs). Our results show that the MI gain spectra consist of only one spectral region instead of one or two regions in ordinary materials, which may be close to or far from the zero point. Particularly, the spectrum far from the zero point has a high cut-off frequency but a narrow spectral width, which is obviously beneficial to the generation of high-repetition-rate pulse trains. Moreover, MI characteristics here will vary with the normalized angular frequency which can be modified by adjusting the structures of negative-refractive MMs, signifying the controllability of bistable solitons and MI based applications. The effects of saturable nonlinearities are similar to those in ordinary materials.

Keywords: modulation instability (MI), negative-refractive metamaterial (MM), saturable nonlinearity, higher-order dispersion

PACS: 42.65.Sf, 42.65.Tg, 42.70.Nq **DOI:** 10.1088/1674-1056/22/3/034205

1. Introduction

In recent years, as important artificial synthetic materials, metamaterials (MMs) have aroused special interests for their extensive potential applications in many fields such as communications, stealth, super resolution imaging, etc. Compared with ordinary materials, MMs are essentially magnetic and structurally adjustable. Thus, the refractive indices of the MMs depend not only on their electric permittivity but also on their magnetic permeability. Correspondingly, according to many previous reports, by adjusting the structure of MMs, one can realize a positive or negative electric response as well as a positive or negative magnetic response. That is to say, one can obtain positive-refractive, negative-refractive, or single-negative (epsilon-negative or mu-negative) materials. It is well-known that they are all very attractive electromagnetic complex materials nowadays. In this work, we are only concerned about the negative-refractive MMs. Current studies on MMs mainly include the realization of negative-refractive materials at different electromagnetic frequency ranges, especially at the optical frequency range, various singular linear and nonlinear physical characteristics, and the exploration of potential applications in a variety of fields.

So far, in the optical frequency range, researchers have investigated nonlinear MMs in terms of the optical propagation of ultra-short optical pulses,[1] second- or third-order harmonic generations, modulation instability (MI),[2–5] and so on. Among them, MI is actually a universal physical phenomenon which can be observed in many nonlinear systems and has all along been an important research topic for its great theoretical and wide-spread practical significance. Theoretically, MI is an important content of nonlinear physics. In particular, it is closely physically related to the soliton generation. Thus, different kinds of MI are generally regarded as precursors of the formation of the corresponding kinds of solitons. Practically, even only in the optics field, MI has already found extensive applications in optical communication systems and the design of all-optical devices, etc. For instance, MI can be typically utilized to generate super-continuum spectra,[6] generate a high repetition rate of ultra-short soliton chains,[7] design optical switching, and so on. However, MI may sometimes be harmful to optical communication systems and high-power laser systems.[8]

Up to now, MI characteristics in optics and its wide-spread applications in ordinary optical materials especially in optical fibers have been extensively investigated theoretically,[9,10] numerically,[7] and experimentally.[11] Besides the lower-order dispersion and nonlinear effects, a variety of higher-order effects such as higher-order dispersion,[12–14] saturable nonlinearity,[13–16] and quintic nonlinearity,[11] have been taken into consideration.

For the reason that the occurrence of MI in new circumstances means new methods to generate and control optical solitons and other new potential applications, MI has been gradually extended to artificial synthetic materials such as photonic crystals and MMs in recent years.[2–5,17–19] Previous studies have revealed that, MI in MMs can occur in the normal dispersion region, without group velocity dispersion, or

*Project supported by the National Key Technology Research and Development Program of the Ministry of Science and Technology of China (Grant No. 210186) and the Scientific Research Foundation of Chengdu University of Information Technology, China (Grant Nos. 2010d1 and J201117).

†Corresponding author. E-mail: zxqlxh@yeah.net

© 2013 Chinese Physical Society and IOP Publishing Ltd

even in the case of anomalous group velocity dispersion and defocusing nonlinearity. For example, Kourakis *et al*.[18] investigated the nonlinear instability in negative-refractive MMs and obtained the MI picture of the coupled plane wave solution. While Wen *et al*. investigated the influence of the self-steepening effect, second-order nonlinear dispersion and fake quintic nonlinearity on MI.[5,19] Malukov *et al*. investigated MI in saturable nonlinear negative-refractive MMs.[3] Xiang *et al*. analytically studied MI in MMs with higher-order linear dispersion and second-order nonlinear dispersion.[20] However, they actually have neglected the effects of higher-order dispersions during calculations. Recently, starting from the normalized propagation equation, Xiang *et al*. further deduced the expressions for the dispersion relation, gain spectra, and the peak gain of MI in negative-refractive MMs and calculated the effects of the saturable nonlinearity, the first- and the second-order nonlinear dispersions on MI.[2] We also investigated effects of exponential saturable nonlinearity and first-order nonlinear dispersion on MI in MMs.[21] However, so far, there are no reports on MI in negative-refractive MMs with both higher-order dispersions and different kinds of saturable nonlinearities.

It is worth mentioning that many previous studies have demonstrated that negative-refractive MMs can be constructed by periodic arrays of split-ring resonators (SRRs) and metallic wires made of copper or gold. If the SRRs are embedded in a nonlinear dielectric, one can construct nonlinear negative-refractive MMs. Furthermore, if the nonlinear dielectric involved has an extremely high nonlinear refractive index and is liable to exhibit the saturable nonlinear effect even for a moderate incident light intensity, the MMs may become the saturable nonlinear ones. On the other hand, the local field enhancements in the SRR arrays can be very intense, which allows for enhanced nonlinear effects, and then makes MMs exhibit saturable nonlinear effects more readily. The typical saturable nonlinear dielectrics include the nonlinear photorefractive material,[3] the semiconductor $CdS_{1-x}Se_x$-doped glass material,[16] and so on. That is to say, embedding the copper or gold SRRs in a certain saturable nonlinear dielectric (the semiconductor $CdS_{1-x}Se_x$-doped glass material, for instance), one can construct a saturable nonlinear negative-refractive MM. Thus, in this work, after taking into account both the higher-order dispersions and three kinds of saturable nonlinearities in negative-refractive MMs, we analytically study and then calculate the MI characteristics by a standard linear stability analysis and the Drude electromagnetic model. Moreover, a comparison of MI characteristics among three kinds of saturable nonlinearities and with those in naturally occurring materials are made in detail.

2. The propagation equation and its coefficients

After taking into account the higher-order dispersions and three kinds of saturable nonlinearity,[16] and referring to the method of the establishment of the nonlinear propagation equation in MMs,[2,5] one can obtain the following extended nonlinear propagation equation

$$\frac{\partial A}{\partial z} = -\frac{\mathrm{i}}{2}\beta_2\frac{\partial^2 A}{\partial T^2} + \frac{1}{6}\delta_3\frac{\partial^3 A}{\partial T^3} + \frac{\mathrm{i}}{24}\delta_4\frac{\partial^4 A}{\partial T^4} + \mathrm{i}\gamma_0 A f(|A|^2), \tag{1}$$

where the function $f(|A|^2)$ stands for a certain kind of saturable nonlinearity. As Ref. [11] has pointed out, three kinds of saturable nonlinearities exist. For convenience, we will call them conventional saturable nonlinearity (CSN), exponential saturable nonlinearity (ESN), and another kind of saturable nonlinearity (ASN), respectively. Their corresponding functions $f(|A|^2)$ in Eq. (1) can be, respectively, expressed as

$$f(|A|^2) = \begin{cases} |A|^2/(1+\Gamma|A|^2), \\ [1-\exp(-\Gamma|A|^2)]/\Gamma, \\ |A|^2(2+\Gamma|A|^2/2)/[2(1+\Gamma|A|^2/2)^2]. \end{cases} \tag{2}$$

The parameters β_2, δ_j $(j=3,4)$, γ_0, $\Gamma = 1/P_{\mathrm{sat}}$, P_{sat}, A, T, and z in Eq. (1) or Eq. (2) are the second-order group-velocity dispersion, the jth-order group-velocity dispersion, the nonlinear coefficient, the saturable parameter, the saturable optical power, the slowly varying amplitude of the optical field, the pulse time coordinate, and the propagation distance, respectively. It is necessary to mention that, although the propagation equation (1) is the same as that in naturally occurring materials in the aspect of its mathematical form, the definitions of the equation coefficients in MMs are quite different from those in naturally occurring materials, and can be found in Ref. [2]. Moreover, the electromagnetic characteristics of MMs are also special and should be described by the Drude electromagnetic model.[22]

Thus, according to the definitions of the propagation equation coefficients and the Drude electromagnetic model, we can deduce the refractive index $n(\omega_0)$ at the carrier angular frequency $\omega_0$and the other equation coefficients as follows:

$$n(\omega_0) = \sqrt{1-\omega_{\mathrm{pe}}^2/\omega_0^2}\sqrt{1-\omega_{\mathrm{pm}}^2/\omega_0^2}, \tag{3}$$

$$\beta_2 = \frac{1}{cn\omega_0}\left[\left(1+3\omega_{\mathrm{pm}}^2\omega_{\mathrm{pe}}^2/\omega_0^4\right) - \frac{1}{n^2}\left(1-\omega_{\mathrm{pm}}^2\omega_{\mathrm{pe}}^2/\omega_0^4\right)^2\right], \tag{4}$$

$$\delta_3 = -\frac{12\omega_{\mathrm{pe}}^2\omega_{\mathrm{pm}}^2}{nc\omega_0^6}, \quad \delta_4 = \frac{60\omega_{\mathrm{pe}}^2\omega_{\mathrm{pm}}^2}{nc\omega_0^7},$$

$$\gamma_0 = \frac{\chi^{(3)}\omega_0}{2nc}\left(1-\omega_{\mathrm{pm}}^2/\omega_0^2\right), \tag{5}$$

where ε_0, μ_0, c, $\chi^{(3)}$, ω_{pe}, and ω_{pm} are the vacuum permittivity, vacuum magnetic permeability, the light speed in a vacuum, the third-order electric susceptibility, the electric and magnetic plasmas angular frequencies, respectively. The susceptibility $\chi^{(3)} > 0$ and $\chi^{(3)} < 0$ represent the self-focusing and self-defocusing nonlinearity, respectively. We can see from Eqs. (3)–(5) that these parameters are related to the normalized angular frequency ω_0/ω_{pe} and cannot vary independently. Thus, the variation of the refractive index n with the normalized angular frequency ω_0/ω_{pe} is shown in Fig. 1. Furthermore, in order to measure these coefficients in MMs in future experiments conveniently, variations of the coefficients of Eq. (1) in real units with the normalized angular frequency ω_0/ω_{pe} for $\omega_{pe} = 600$, 800, and 1000 THz are shown in Figs. 2–5. The common parameters have been set as $\omega_{pm}/\omega_{pe} = 0.8$ and $\chi^{(3)} = 10^{-10}$ esu. during calculations.[23]

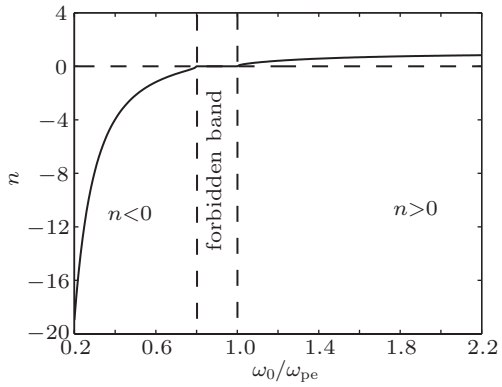


Fig. 1. Variation of the refractive index n with the normalized angular frequency ω_0/ω_{pe}.

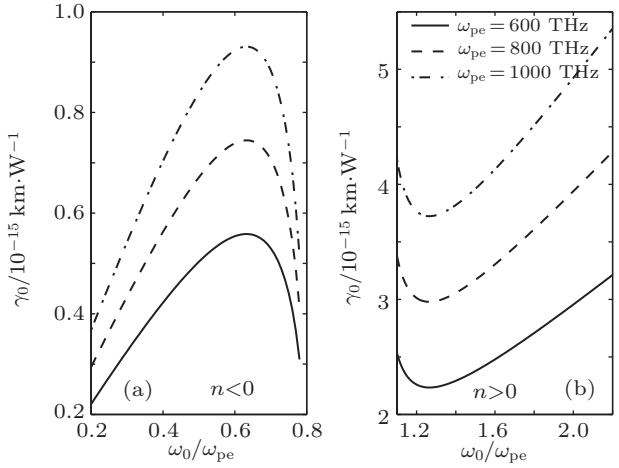


Fig. 2. Variation of the equation coefficient γ_0 with the normalized angular frequency ω_0/ω_{pe} for $\omega_{pm}/\omega_{pe} = 0.8$ and $\omega_{pe} = 600$, 800, and 1000 THz, in the (a) negative and (b) positive refractive region, respectively.

Obviously, we can see from Fig. 1 that, the frequency regions $0 < \omega_0/\omega_{pe} < 0.8$, $0.8 < \omega_0/\omega_{pe} < 1$, and $\omega_0/\omega_{pe} > 1$ are the negative refractive region, the forbidden band region, and the positive refractive region, respectively. In the forbidden band region, the refractive index becomes a purely imaginary number, which indicates that, according to Eqs. (4) and (5), all of the equation coefficients γ_0, β_2, δ_3, and δ_4 will correspondingly become complex and physically meaningless. For this reason, in Figs. 2–5, we only show the cases in the negative and positive refractive regions. These figures indicated that, in the negative refractive region, with the increase of ω_0/ω_{pe}, the parameters n and δ_4 increase monotonically and tend to be zero, γ_0 first increases and then increases, β_2 first increases from negative to zero slowly and then increases rapidly near the forbidden band region, and δ_3 decreases monotonically and tends to be zero. When the other parameters are the same, the larger parameter ω_{pe} is, the larger parameters γ_0, δ_4, and β_2 (far from the forbidden band region) are, and the smaller parameter δ_3 is. While in the positive refractive region, with the increase of ω_0/ω_{pe}, n increases monotonically, β_2 and δ_3 increase monotonically and tend to be zero, δ_4 decreases monotonically and tends to be zero, and γ_0 first decreases and then increases. When the other parameters are the same, the larger parameter ω_{pe} is, the larger the parameters γ_0, β_2, and δ_3 are, and the smaller parameter δ_4 is.

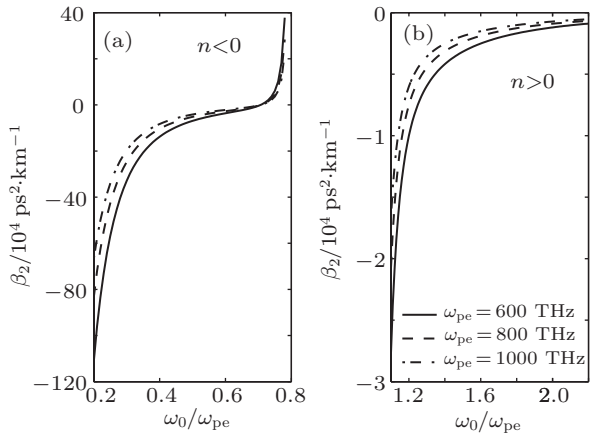


Fig. 3. Variation of the equation coefficient β_2 with the normalized angular frequency ω_0/ω_{pe} for $\omega_{pm}/\omega_{pe} = 0.8$ and $\omega_{pe} = 600$, 800, and 1000 THz, in the (a) negative and (b) positive refractive region, respectively.

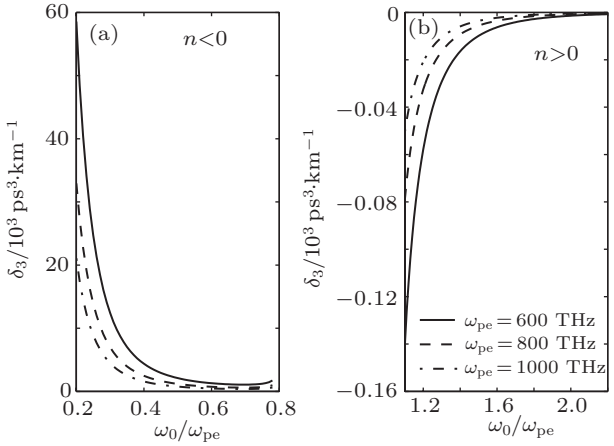


Fig. 4. Variation of the equation coefficient δ_3 with the normalized angular frequency ω_0/ω_{pe} for $\omega_{pm}/\omega_{pe} = 0.8$ and $\omega_{pe} = 600$, 800, and 1000 THz, in the (a) negative and (b) positive refractive region, respectively.

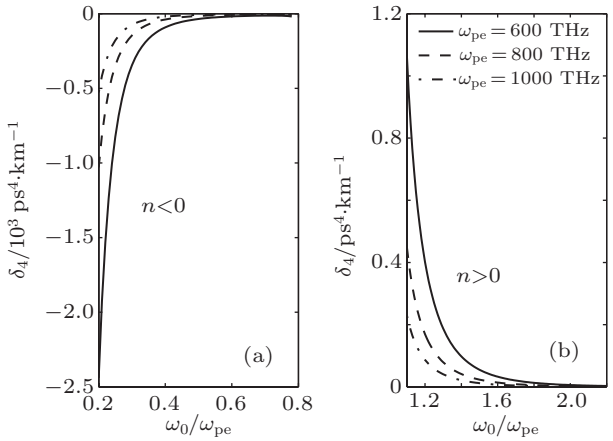


Fig. 5. Variation of the equation coefficient δ_4 with the normalized angular frequency ω_0/ω_{pe} for $\omega_{pm}/\omega_{pe}=0.8$ and $\omega_{pe}=600$, 800, and 1000 THz, in the (a) negative and (b) positive refractive region, respectively.

3. Linear stability analysis

It is easy to obtain the linearized nonlinear propagation equation of Eq. (1) by perturbing its steady-state solution through adding a perturbation $a\,(z,T)$ with angular frequency Ω and utilizing the standard linear stability analysis. This linearized equation can be written as

$$\frac{\partial a}{\partial z} = \mathrm{i}\gamma P_0\,(a+a^*) - \mathrm{i}\frac{\beta_2}{2}\frac{\partial^2 a}{\partial T^2} + \frac{\delta_3}{6}\frac{\partial^3 a}{\partial T^3} + \mathrm{i}\frac{\delta_4}{24}\frac{\partial^4 a}{\partial T^4}, \tag{6}$$

where parameter P_0 is the incident optical power density, and γ is defined as

$$\gamma = \begin{cases} \gamma_0/(1+\Gamma P_0)^2, & (\mathrm{CSN}) \\ \gamma_0 \exp(-\Gamma P_0), & (\mathrm{ESN}) \\ \gamma_0/(1+0.5\Gamma P_0)^3, & (\mathrm{ASN}). \end{cases} \tag{7}$$

According to Eq. (6), one can deduce the following power gain spectrum of MI by utilizing the standard steps of linear stability analysis

$$g\,(\Omega) = \frac{1}{12}|\delta_4\,\Omega|\sqrt{-\left(\Omega^2+12\frac{\beta_2}{\delta_4}\right)\left[\Omega^4+12\frac{\beta_2}{\delta_4}\Omega^2+\frac{48\gamma P_0}{\delta_4}\right]}, \tag{8}$$

where the angular frequency of perturbation is $\Omega=2\pi\nu$, and ν is the frequency. The corresponding instable condition should be

$$\left(\Omega^2-\Omega_1^2\right)\left(\Omega^2-\Omega_2^2\right)\left(\Omega^2-\Omega_3^2\right)<0, \tag{9}$$

where the parameter $\Omega_j=2\pi\nu_j\ (j=1,2,3)$ is defined as

$$\Omega_1^2 = -\frac{12\beta_2}{\delta_4},$$

$$\Omega_{2,3}^2 = \left[-\frac{6\beta_2}{\delta_4} \pm \sqrt{\left(\frac{6\beta_2}{\delta_4}\right)^2 - \frac{48\gamma P_0}{\delta_4}}\right], \tag{10}$$

where the signs '+' and '–' correspond to Ω_2^2 and Ω_3^2, respectively. Parameter Ω_1^2 does not vary with the optical power density P_0.

Obviously, the propagation equation, dispersion relationship, the instable condition, the power gain spectrum, and MI spectral regions are mathematically the same as those in ordinary optical materials with higher-order dispersions.[12] However, due to the different definitions and characteristics of the parameters β_2, δ_3, δ_4, and γ_0, some new features will appear for negative-refractive MMs, which will be demonstrated in the following part, where the MI characteristics will be calculated and discussed.

4. Calculations and discussion

Taking ASN as an example, we have calculated the variations of gain spectra of MI with the parameters ΓP_0 for different normalized angular frequency ω_0/ω_{pe} as shown in Fig. 6. The common parameter is set as $\omega_{pe}=600$ THz so that MMs will operate in the infrared region and can exhibit negative-refractive effects more easily. We can see that all of the gain spectra consists of only one spectral region. However, the spectrum may be close to or far from the zero point, as shown in Figs. 6(a) and 6(b), respectively, which is easy to be interpreted. Actually, we can see from Figs. 4 and 5 that there are two sign combinations of β_2 and δ_4 in the negative-refractive

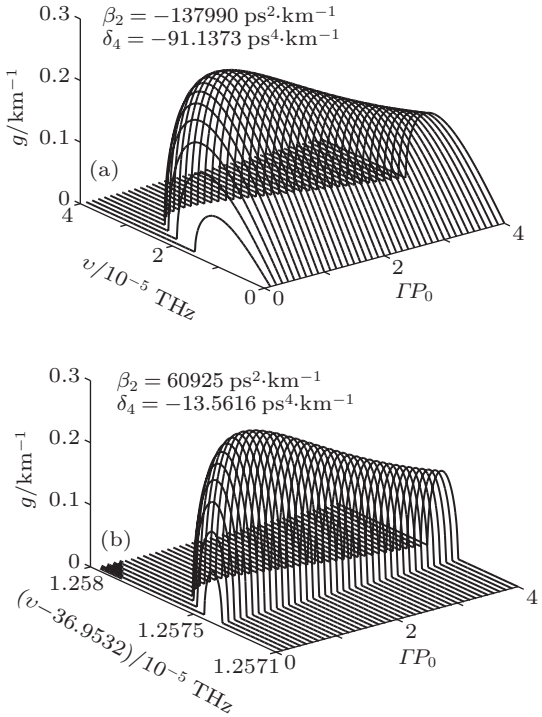


Fig. 6. Variations of gain spectra of MI with the parameters ΓP_0 for (a) $\omega_0/\omega_{pe}=0.4$ and (b) $\omega_0/\omega_{pe}=0.75$ in the case of ASN.

MMs. They are $\beta_2 < 0$ and $\delta_4 < 0$ for small values of ω_0/ω_{pe}, and $\beta_2 > 0$ and $\delta_4 < 0$ for large values of ω_0/ω_{pe}, respectively. According to Eqs. (9) and (10), the corresponding spectral regions should be $0 < \Omega^2 < \Omega_2^2$ and $\Omega_1^2 < \Omega^2 < \Omega_2^2$, respectively. With the increase of ω_0/ω_{pe}, the gain spectrum transfers from $0 < \Omega^2 < \Omega_2^2$ to $\Omega_1^2 < \Omega^2 < \Omega_2^2$, and shifts toward the high frequency region, where Ω_1^2 does not vary with ΓP_0. Furthermore, the larger the value of ω_0/ω_{pe} is, the higher the cut-off angular frequencies Ω_2 are, and the wider the gain band widths Ω_2 or $\Omega_2^- \Omega_1$ will be. These characteristics can be seen more clearly in Figs. 7(a), 8, and 9(a), which is undoubtedly beneficial to generate high-repetition-rate optical pulse chains useful for high-speed optical communication systems.

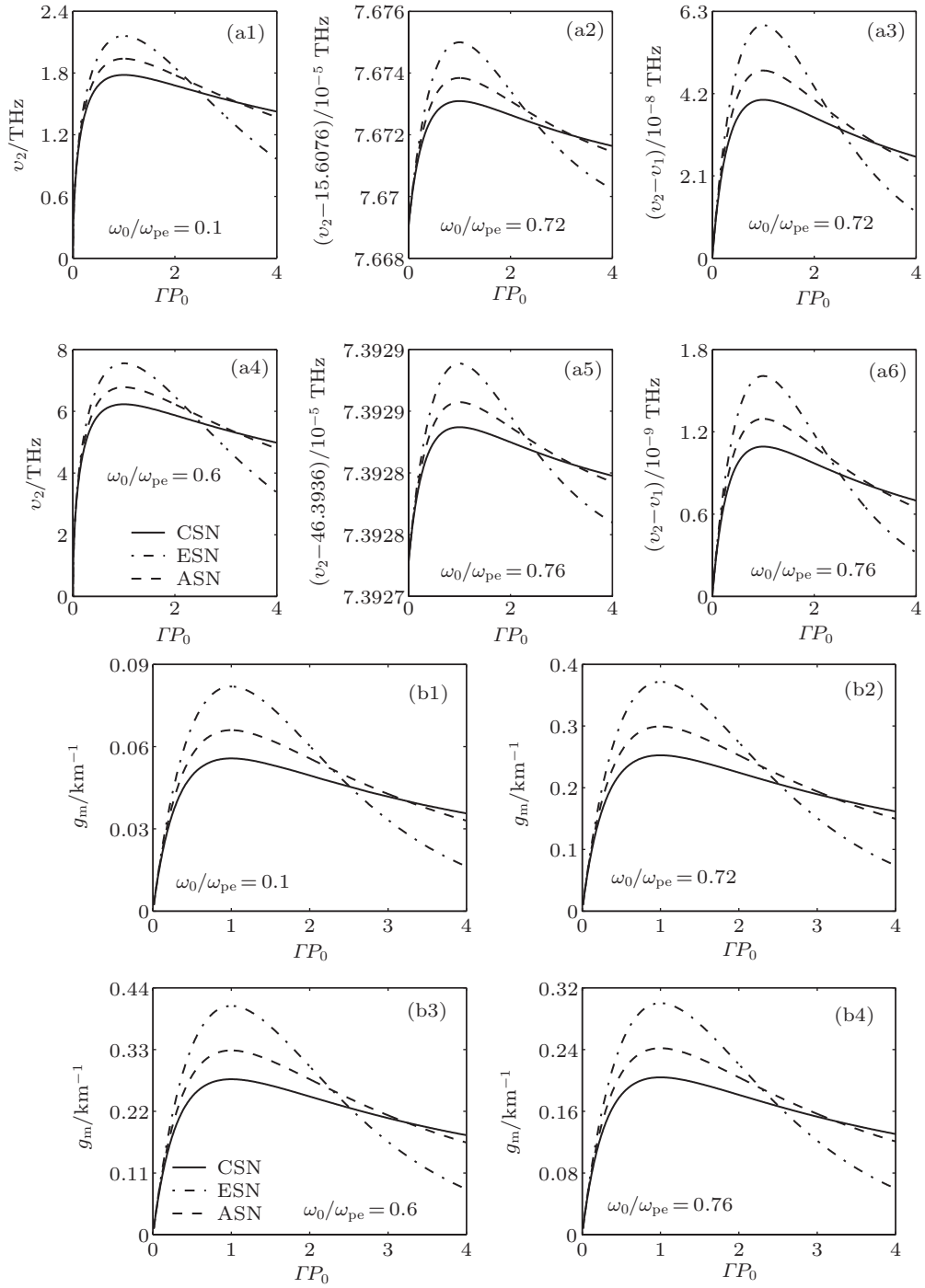


Fig. 7. Variations of (a1)–(a6) cut-off frequencies υ_2, spectral widths $\upsilon_2 - \upsilon_1$, and (b1)–b(4) peak gains g_m with ΓP_0 for different normalized frequencies ω_0/ω_p for ESN (dash-dotted line), CSN (solid line), and ASN (dashed line).

In addition, Figure 7 also shows that, when ω_0/ω_{pe} is fixed, with the increase of ΓP_0, the cut-off angular frequencies Ω_2, the gain band widths Ω_2 or $\Omega_2 - \Omega_1$, and the peak gain g_m will all increase and then decrease. The ESN (CSN) has the largest (smallest) values of cut-off angular frequencies Ω_2, the gain band widths Ω_2 or $\Omega_2 - \Omega_1$, and the peak gain g_m. However, when ΓP_0 is fixed, with the increase of ω_0/ω_{pe}, the peak gain will first increase, and then decrease, as shown in Fig. 9(b).In addition , depending on different values of ΓP_0, the size relationship and differences of the cut-off angular frequencies Ω_2, the gain band widths Ω_2 or $\Omega_2 - \Omega_1$, and the peak gain g_m among the three kinds of nonlinearities are also different, which can also be seen from Fig. 9. Here, it is necessary to mention that, according to Figs. 2–5 and Eqs. (3)–(5), we can make sure that the coefficients of the propagation equation (1) are all closely related to the normalized angular frequency ω_0/ω_{pe} and cannot vary independently. Thus, variations of MI gain spectra, cut-off frequencies, and peak gains, with the normalized angular frequencies instead of each independent coefficient of Eq. (1) are calculated above, as shown in Figs. 8 and 9.

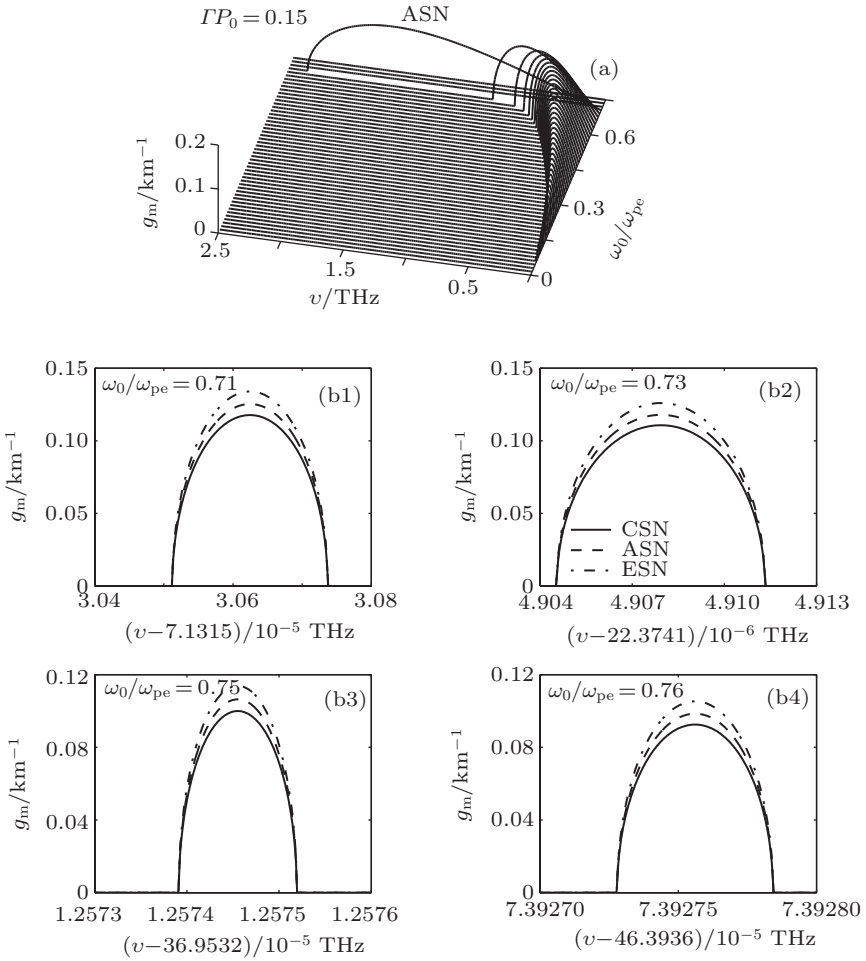


Fig. 8. (a) Variations of gain spectra with the normalized frequencies ω_0/ω_{pe} for $\Gamma P_0 = 0.15$. Variation of the peak gain g_m with (b1) $(\nu - 7.1375)/10^5$, (b2) $(\nu - 22.3741)/10^6$, (b3) $(\nu - 36.9532)/10^5$, and (b4) $(\nu - 46.3936)/10^5$.

By comparison, the effects of saturable nonlinearity on MI in negative-refractive MMs are similar to those in ordinary saturable nonlinear optical materials.[14,15] However, the gain spectra here consist of only one spectral region instead of one or two spectral regions in ordinary optical materials with higher-order dispersions.[12] Moreover, MI characteristics in saturable nonlinear negative-refractive MMs will vary with the normalized angular frequency ω_0/ω_{pe} and can be modified effectively by adjusting their structures.

It is worth mentioning that we have also calculated the MI characteristics when the value of ω_{pe} is set to be larger or smaller than 600 THz and found that the overall law of MI remains unchanged.

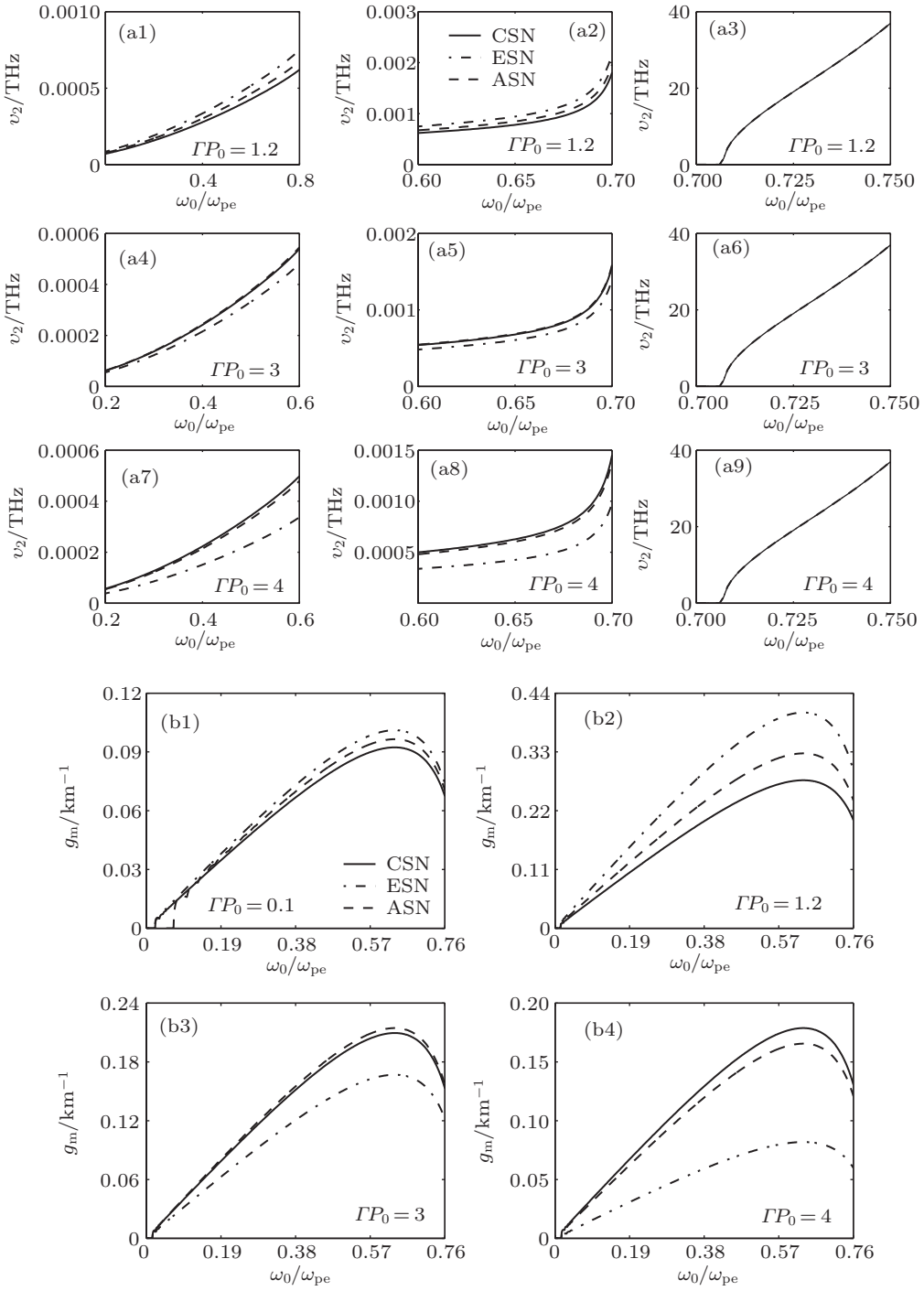


Fig. 9. Variations of (a) cut-off frequencies υ_2 and (b) peak gains g_m with ω_0/ω_p for different ΓP_0 for ESN (dash-dotted line), CSN (solid line), and ASN (dashed line).

5. Conclusions

In summary, based on the standard linear stability analysis and the extended nonlinear propagation equation including the higher-order dispersions and three kinds of saturable nonlinearities, MI characteristics have been analyzed and calculated in detail. Our results show that, the propagation equation, dispersion relationship, instable condition, power gain spectrum, and MI spectral regions in saturable nonlinear negative-refractive MMs are revealed to be mathematically the same as those in ordinary materials. However, due to its special electromagnetic characteristics described by the Drude model, the propagation equation coefficients, gain spectra, the corresponding cut-off frequencies, gain band widths, and peak gains, are all closely related to the normalized angular frequencies. Thus, MI characteristics in saturable nonlinear negative-refractive MMs and their corresponding applications can be modified effectively by adjusting the structures of MMs to modify their electric and magnetic plasmas angular frequen-

cies and then their normalized angular frequencies. The adjustability of MI also means the controllability of solitons, even the bistable ones and other corresponding applications of MI. Furthermore, in comparison with that in ordinary materials with a higher-order dispersion, the MI gain spectra here consist of only one spectral region instead of one or two spectral regions. The spectral regions which are far away from the zero point have much higher perturbation frequencies but narrow spectral widths, which is of great importance for generating high-repetition-rate soliton pulse chains utilized for high-speed communication systems. Moreover, the soliton pulse chains with adjustable repetition rate here can thus be applied for communication systems with different speed demands. However, the effects of saturable nonlinearity on MI are similar to those in ordinary saturable materials. In addition, when the other parameters are the same, ESN (CSN) has a larger (smaller) gain band width and peak gain, and then it is more beneficial (detrimental) to generate MI. Thus, one can select negative-refractive MMs with ESN to improve corresponding applications such as the generation of soliton pulse chains, the supercontinuum, optical switches, and so on.

References

[1] Cui W N, Zhu Y Y, Li H X and Liu S M 2009 *Phys. Lett. A* **374** 380
[2] Xiang Y J, Dai X Y, Wen S C and Fan D Y 2011 *J. Opt. Soc. Am. B* **28** 908
[3] Maluckov A, Hadžievski Lj, Lazarides N and Tsironis G P 2008 *Phys. Rev. E* **77** 046607
[4] Dai X Y, Wen S C and Xiang Y J 2008 *Acta Phys. Sin.* **57** 186 (in Chinese)
[5] Wen S C, Xiang Y J, Su W H, Hu Y H, Fu X Q and Fan D Y 2006 *Opt. Express* **14** 1568
[6] Demircan A and Bandelow U 2006 *Appl. Phys. B* **86** 31
[7] Zhong X Q and Xiang A P 2010 *Chin. Phys. Lett.* **27** 014203
[8] Alexander M, Rubenchik M, Turitsyn K and Fedoruk M P 2010 *Opt. Exptress* **18** 1380
[9] Choudhuri A and Porsezian K 2012 *Phys. Rev. A* **85** 033820
[10] Wen S C, Su W H, Zhang H, Fu X Q, Qian L J and Fan D Y 2003 *Chin. Phys. Lett.* **20** 852
[11] Cheng W, Meng Z and Zhou H J 2012 *Chin. Phys. B* **21** 094215
[12] Abdullaev F Kh, Darmanyan S A, Bischoff S, Christiansen P L and Sørensen M P 1994 *Opt. Commun.* **108** 60
[13] Zhong X Q and Xiang A P 2010 *Chin. Phys. B* **19** 064212
[14] Dinda P and Porsezian K 2010 *J. Opt. Soc. Am. B: Opt. Phys.* **27** 1143
[15] Hickmann J M, Cavalcanti S B, Borges N M, Gouveia E A and Gouveia-Neto A S 1993 *Opt. Lett.* **18** 182
[16] Lyra M L and Gouveia-Neto A S 1994 *Opt. Commun.* **108** 117
[17] Amarendra K S and Manirupa S 2011 *J. Opt. Soc. Am. B: Opt. Phys.* **28** 944
[18] Kourakis I and Shukla P K 2005 *Phys. Rev. E* **72** 016626
[19] Wen S C, Wang Y W, Su W H, Xiang Y J, Fu X Q and Fan D Y 2006 *Phys. Rev. E* **73** 036617
[20] Xiang Y J, Wen S C, Dai X Y, Tang Z X, Su W H and Fan D Y 2007 *J. Opt. Soc. Am. B: Opt. Phys.* **24** 3058
[21] Zhong X Q, Tang T T, Xiang A P and Cheng K 2011 *Opt. Commun.* **284** 4727
[22] Pendry J B 2000 *Phys. Rev. Lett.* **85** 3966
[23] Zhou W, Su W H, Cheng X, Xiang Y J, Dai X Y and Wen S C 2009 *Opt. Commun.* **282** 1440